ARTICLE

OBC
www.rsc.org/obc

Creation of hydrogen bonded 1D networks by co-crystallization of *N*,*N*′-bis(2-pyridyl)aryldiamines with dicarboxylic acids †

Igor Bensemann,[a] Maria Gdaniec,*[b] Karina Łakomecka,[b] Maria J. Milewska[a] and Tadeusz Połoński*[a]

[a] *Department of Chemistry, Technical University, 80-952 Gdańsk, Poland. E-mail: tadpol@chem.pg.gda.pl*

[b] *Faculty of Chemistry, A. Mickiewicz University, 60-780 Poznań, Poland. E-mail: magdan@amu.edu.pl*

Received 26th November 2002, Accepted 26th February 2003
First published as an Advance Article on the web 18th March 2003

The preparation and crystal structures of fourteen complexes of *N*,*N*′-bis(2-pyridyl)aryldiamines with dicarboxylic acids and two complexes with squaric acid are reported. The recognition between the carboxylic acids and the 2-aminopyridine units occurs through the formation of the cyclic R^2_2 (8) hydrogen bond motif, whereas squaric acid creates the analogous R^2_2 (9) motif. In the 1 : 1 complexes the cyclic motifs generate infinite hydrogen-bonded 1D networks with the alternating component molecules. These networks are further organised into densely packed layers assembled through weaker C–H ··· O interactions. Analysis of the intermolecular interactions in these complexes led us to the synthesis of *N*,*N*′-bis(2-pyridyl)-2,2′-oxybis(aminobenzene) (**5**) which acts as a tritopic receptor of the carboxylic group and forms exclusively 2 : 1 complexes with dicarboxylic acids.

Introduction

The design and preparation of ordered solid-state structures by means of specific intermolecular interactions is an area of crystal engineering.[1] This rapidly expanding branch of supramolecular chemistry offers a possibility for rational development of new materials with potentially useful physical and chemical properties.[2] A considerable progress has been made in recent years in controlling the assembly of individual molecules into extended arrays of various dimensionalities in a pre-determined fashion. Particularly hydrogen bonds as directional and strong intermolecular interactions offer a powerful tool to control solid-state structures.[1,3] Thus far, many hydrogen bonding patterns that can be used for a manipulation of the spatial arrangement of molecules in the solid-state have been identified and reported.[4]

Recently, we have shown that hydrogen bonded *N*,*N*′-bis-(2-pyridyl)aryldiamines are able to form 1D networks by the cyclic $R^2_2(8)$ motif **I**.[5,6] However, due to a low energy barrier to C–N rotation, the 2-arylaminopyridine system can adopt either (*Z*) or (*E*) conformations giving rise to the formation of conformational polymorphs. Indeed, in several cases, besides the aforementioned motif **I**, we were able to isolate the second crystalline form, polymorph or solvate, where the 2-arylaminopyridine monomeric units assumed the (*Z*) conformation and the molecules were assembled *via* a catemeric C(4) motif into 1D, 2D or even 3D networks.[5] Since the conformational polymorphism significantly reduces the level of predictability of the supramolecular structures it would be desirable to restrict the conformational space available to molecules in crystals by choosing specific, strong non-covalent interactions which would significantly limit the number of possible conformers. The solid-state molecule-based architectures can be constructed by self-assembly not only of one but also two or more components and the co-crystallization of selected molecules bearing complementary functional groups may generate well defined extended supramolecular frameworks.[7] It is well known that the 2-aminopyridine function is capable of forming cyclic R^2_2 (8) hydrogen bond motifs **IIa,b** with the carboxyl group[8] and furthermore, in the solid state it prefers to bind to the carboxyl group rather than to itself.[4a,9] Therefore the robust motif **IIa** formed by *N*-acyl-2-aminopyridines or 2-aminopyrimidines and carboxylic acids have been frequently utilized for crystal engineering.[9] We expected that this kind of cyclic complexation should force the 2-aminopyridine units in the title compounds to adopt the (*E*) conformation and hence direct the aggregation process towards the desired 1D networks shown in Scheme 1. In the present study, we report the preparation and crystal structure determination of the hydrogen bonded heteromeric systems formed by *N*,*N*′-bis(2-pyridyl)aryldiamines **1**–**5** with several aliphatic and aromatic dicarboxylic acids, which include oxalic (**oxa**), malonic (**mal**), succinic (**suc**), sebacic (**seb**), fumaric (**fum**), isophthalic (**iso**), terephthalic (**tere**), diphenic (**diph**) and 4,4′-oxybisbenzoic (**obe**) acids.

In addition we tested the utility of squaric acid (3,4-dihydroxy-3-cyclobutene-1,2-dione) (**sq**) for complexation of *N*,*N*′-bis(2-pyridyl)aryldiamines. Interaction of this strong

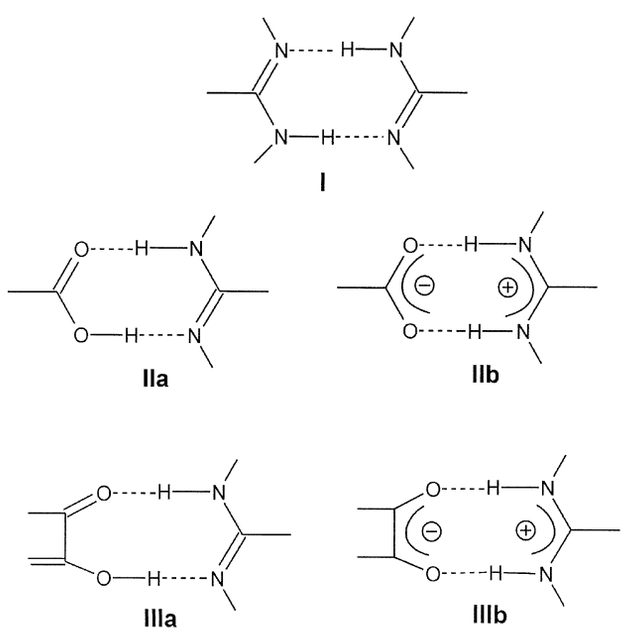

† Supramolecular structures formed by 2-aminopyridine derivatives. Part II.[5]

DOI: 10.1039/b211675h

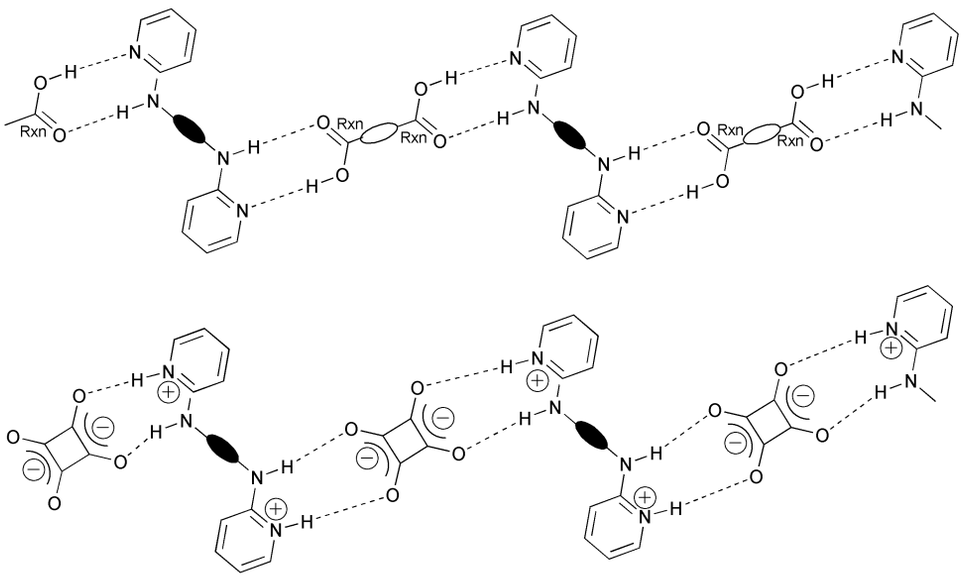

Scheme 1

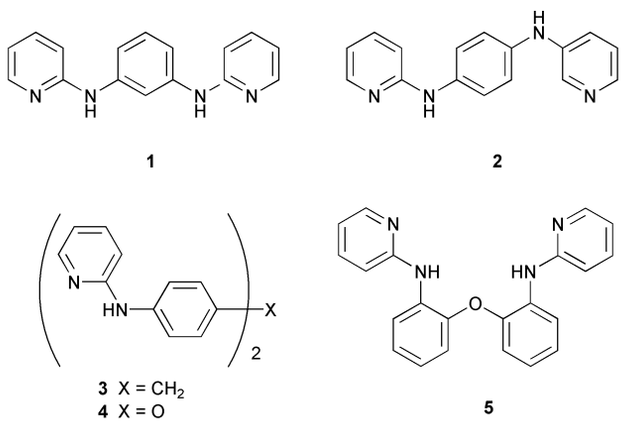

dibasic acid with the 2-aminopyridine function could lead to the cyclic $R^2_2(9)R^2_2(9)$ motifs **IIIa,b** and creation of supramolecular networks that are possibly stiffer than those formed by dicarboxylic acids.[10]

Results and discussion

Diffraction quality crystals of the molecular complexes were prepared by co-crystallization of the two components, a dicarboxylic acid and *N*,*N*′-bis(2-pyridyl)aryldiamine, in a 1 : 1 molar ratio from ethanol at ambient temperature. The complexes of squaric acid were crystallized from ethanol–water. In four cases (**1_2·tere**, **3_2·tere**, **5_2·fum** and **5_2·tere**), despite the equimolar ratio of the components used, the 2 : 1 adducts were obtained. Co-crystallization of structurally related compounds **3** and **4** with terephthalic acid yielded solvated complexes **3_2·tere·(EtOH)$_2$** and **4·tere·H_2O**, respectively.

Table 1 summarises the details of X-ray crystallographic analyses for the sixteen examined complexes. In all structures except **4·tere·H_2O**, the space group imposes symmetry on at least one molecular component of the crystal. In the 1 : 1 complexes formed by **1** the bis-pyridylamine has crystallographically imposed mirror symmetry whereas dicarboxylic acids are located at special positions of C_i (**1·oxa**, **1·suc**, **1·seb** **1·sq)** or C_2 symmetry (**1·iso**, **1·obe**). In effect, an asymmetric part of the unit cell contains one half of the molecule of **1** and one half of the acid molecule. In **1_2·tere**, the terephthalic dianion lies about a center of symmetry and the monocation of **1** occupies a general position. A similar trend of occupying special positions by the component molecules is shown by the complexes of **2**, where the bis-pyridylamine has crystallographic C_i symmetry and dicarboxylic acids are located at a 2-fold axis (**2·diph**, **2·mal)** or around an inversion center (**2·sq**, **2·tere**). In **2·seb** two symmetry independent molecules of **2** are situated at special positions whereas the sebacic acid molecule is found in a general position. On the other hand, inspection of the complexes of **5** with a 2 : 1 stoichiometry and **3_2·tere·(EtOH)$_2$** revealed the bis-pyridylamine in a general position and the dicarboxylic acid occupying a special position of C_i symmetry.

The geometry of hydrogen bonds is listed in Table 2. The O ··· N hydrogen bond distances, where N is the pyridine nitrogen, fall in the range of 2.53–2.68 Å indicating strong hydrogen bonds. For comparison, the O ··· N distances in the N–H ··· O hydrogen bonds formed by the 2-aminopyridine N–H group are in the range of 2.70–3.00 Å, with the lowest values observed for the complexes of squaric acid.

Some useful supplemental information about hydrogen bonding in these systems was provided by the solid state IR spectra. The neutral character of the first group of the dicarboxylic acid complexes (**1·iso**, **1·suc**, **1·seb**, **1·obe**, **2·seb** and **2·diph**) is reflected by two broad bands of moderate intensities near 2400 and 1900 cm^{-1}. They are due to the O–H stretching vibrations (ν_{OH}) in the carboxylic group bonded to the pyridine nitrogen.[11] The ν_{CO} stretching near 1680 cm^{-1} occurs at a frequency *ca.* 10–20 cm^{-1} lower than that in the parent acids which points to strong hydrogen bonding of the carbonyl group. On the other hand, the spectra of the second group of the co-crystals including: **1_2·tere**, **2·tere**, **2·mal** and **3_2·tere·(EtOH)$_2$** show a strong broad band centered near 2950 cm^{-1} or, as in the case of **1·oxa**, at 2650 cm^{-1} in addition to two weaker ones at 2450 and 1950 cm^{-1}. Apparently the high frequency strong absorption can be attributed to the N–H stretching vibrations (ν_{NH}) of the protonated pyridine nitrogen. These compounds reveal also two equal intensity ν_{CO} bands near 1600 and 1350 cm^{-1} corresponding to the carboxylic anion. Analogously, the squaric acid adducts **1·sq** and **2·sq** exhibit a strong broad band at 2585 cm^{-1} accompanied by a weaker one at 1980 cm^{-1}. Some complexes (**4·tere·H_2O**, **5_2·fum** and **5_2·tere**) reveal three broad bands of moderate intensity near 2950, 2450 and 1550 cm^{-1}, indicating an intermediate character of the complexes.

The crystallographic data confirm the neutral character of the complexes **1·iso**, **1·suc**, **1·seb**, **1·obe**, **2·seb** and **2·diph**. In their crystal structures, the carboxylic hydrogens, positions of which were found from the difference Fourier maps and fully refined, are unequivocally linked to the oxygens since the O–H distances are in range of 0.99–1.10 Å. Furthermore, the lengths of the two carboxylic C–O bonds differ by more than 0.8 Å and

Table 1 X-Ray structure determination summary

Crystal data	**1·iso**	**1·obe**	**1·oxa**	**1·seb**	**1·sq**	**1·suc**
Chemical formula moiety	$C_{16}H_{14}N_4{\cdot}C_8H_6O_4$	$C_{16}H_{14}N_4{\cdot}C_{14}H_{10}O_5$	$C_{16}H_{14}N_4{\cdot}C_2H_2O_4$	$C_{16}H_{14}N_4{\cdot}C_{10}H_{18}O_4$	$C_{16}H_{14}N_4{\cdot}C_4H_2O_4$	$C_{16}H_{14}N_4{\cdot}C_4H_6O_4$
Formula weight	428.44	520.53	352.35	464.56	376.37	380.4
T/K	296	100	296	130	100	294
Crystal size/mm	0.4 × 0.4 × 0.2	0.2 × 0.15 × 0.1	0.4 × 0.1 × 0.01	0.7 × 0.2 × 0.02	0.2 × 0.08 × 0.01	0.65 × 0.35 × 0.05
Crystal system	Orthorhombic	Orthorhombic	Orthorhombic	Monoclinic	Orthorhombic	Monoclinic
Space group	*Pbcm*	*Ama*2	*Pnma*	$P2_1/m$	*Pnma*	$P2_1/m$
a/Å	9.1922(11)	35.743(7)	7.281(3)	5.4920(10)	7.251(4)	5.7015(5)
b/Å	7.1341(11)	9.285(2)	24.097(6)	34.585(2)	24.325(5)	26.821(3)
c/Å	31.750(4)	7.3380(10)	8.919(3)	6.3180(10)	9.185(3)	6.1015(6)
α°						
β°				102.810(10)		104.708(8)
γ°						
V/Å^3	2082.1(5)	2435.3(8)	1564.8(5)	1170.2(3)	1620.1(11)	902.47(16)
Z	4	4	4	2	4	2
λ/Å	0.71073 (MoK_α)	0.71073 (MoK_α)	1.54178 (CuK_α)	0.71073 (MoK_α)	0.71073 (MoK_α)	1.54178 (CuK_α)
μ/mm^{-1}	0.095	0.099	0.904	0.090	0.111	0.824
Total reflections	10774	3651	2182	6765	7085	2346
Independent reflections (R_{int})	1867 (0.071)	1135 (0.055)	1274 (0.027)	2024 (0.059)	1281 (0.158)	1533 (0.020)
R_1, wR_2 [$I>2\sigma(I)$]	0.0666, 0.1534	0.0371, 0.0788	0.0352, 0.0785	0.0561, 0.1135	0.0838, 0.1717	0.0372, 0.1011
R_1, wR_2 (all data)	0.0701, 0.1577	0.0550, 0.0836	0.0853, 0.0853	0.0811, 0.1293	0.1333, 0.2047	0.0453, 0.1064

Crystal data	**1_2·tere**	**2·diph**	**2·mal**	**2·seb**	**2·sq**	**2·tere**
Chemical formula moiety	$C_{16}H_{14}N_4{\cdot}0.5(C_8H_6O_4)$	$C_{16}H_{14}N_4{\cdot}C_{14}H_{10}O_4$	$C_{16}H_{14}N_4{\cdot}C_3H_4O_4$	$C_{16}H_{14}N_4{\cdot}C_{10}H_{18}O_4$	$C_{16}H_{14}N_4{\cdot}C_4H_2O_4$	$C_{16}H_{14}N_4{\cdot}C_8H_6O_4$
Formula weight	345.38	504.53	366.37	464.56	376.37	428.44
T/K	294	296	296	294	100	294
Crystal size/mm	0.4 × 0.4 × 0.4	0.5 × 0.4 × 0.2	0.35 × 0.1 × 0.06	0.3 × 0.2 × 0.01	0.3 × 0.1 × 0.01	0.7 × 0. 5 × 0.1
Crystal system	Monoclinic	Orthorhombic	Monoclinic	Triclinic	Triclinic	Triclinic
Space group	$P2_1/n$	*Pbcn*	*C*2/*c*	P$\bar{1}$	P$\bar{1}$	P$\bar{1}$
a/Å	10.268(2)	9.117(2)	17.290(2)	8.4312(9)	3.8420(10)	7.7670(13)
b/Å	10.529(3)	14.433(4)	4.0427(5)	10.1438(12)	9.062(2)	8.8044(17)
c/ Å	11.158(2)	19.312(6)	24.720(3)	15.0064(15)	12.098(2)	9.1959(17)
α/°				85.842(9)	87.23(3)	62.048(19)
β/°	105.47(3)		93.121(11)	73.025(9)	81.25(3)	71.921(17)
γ/°				78.006(9)	78.18(3)	70.707(16)
V/Å^3	1714.7(6)	2541.2(12)	1725.3(4)	1200.6(2)	407.41(15)	515.10(16)
Z	4	4	4	2	1	1
λ/Å	0.71073 (Mo K_α)	0.71073 (Mo K_α)	1.54178 (Cu K_α)	0.71073 (Mo K_α)	0.71073 (Mo K_α)	1.54178 (Cu K_α)
μ/mm^{-1}	0.090	0.089	0.841	0.088	0.110	0.792
Total reflections	12805	2258	2040	9211	3082	1621
Independent reflections (R_{int})	3016 (0.020)	2258	1374(0.28)	4194 (0.058)	1442 (0.035)	1621
R_1, wR_2 [$I>2\sigma(I)$]	0.0406, 0.1168	0.0398, 0.0977	0.0345, 0.0871	0.0565, 0.1004	0.0510, 0.0960	0.0466, 0.1237
R_1, wR_2 (all data)	0.0500, 0.1235	0.1369, 0.1129	0.0657, 0.0986	0.1829, 0.1302	0.0693, 0.1074	0.0546, 0.1275

Crystal data	**3_2·tere·(EtOH)$_2$**	**4·tere·H$_2$O**	**5_2·fum**	**5_2·tere**
Chemical formula moiety	$C_{23}H_{20}N_4{\cdot}0.5\,(C_8H_6O_4){\cdot}C_2H_5OH$	$C_{22}H_{18}N_4O{\cdot}C_8H_6O_4{\cdot}H_2O$	$C_{22}H_{18}N_4O{\cdot}0.5(C_4H_4O_4)$	$C_{22}H_{18}N_4O{\cdot}0.5(C_8H_6O_4)$
Formula weight	481.56	538.55	412.44	437.47
T/K	294	294	294	294
Crystal size/mm	0.25 × 0.25 × 0.06	0.4 × 0.4 × 0.3	0.4 × 0.4 × 0.3	0.5 × 0.4 × 0.07
Crystal system	Triclinic	Triclinic	Monoclinic	Triclinic
Space group	P$\bar{1}$	P$\bar{1}$	*C*2/*c*	P$\bar{1}$
a/Å	8.7830(11)	10.3442(7)	28.8097(18)	8.2875(6)
b/Å	10.6035(11)	11.7028(9)	7.8866(6)	10.1511(8)
c/Å	13.8087(15)	12.6687(9)	18.5925(10)	13.3739(10)
α/°	88.060(9)	78.461(6)		78.828(7)
β/°	87.645(9)	65.910(6)	98.004(5)	87.705(6)
γ/°	86.861(9)	73.925(6)		84.019(6)
V/Å^3	1282.4(3)	1338.68(17)	4183.3(5)	1097.55(14)
Z	2	2	8	2
λ/Å	0.71073 (MoK_α)	0.71073 (MoK_α)	0.71073 (MoK_α)	0.71073 (MoK_α)
μ/mm^{-1}	0.082	0.096	0.089	0.089
Total reflections	9437	10143	9500	7973
Independent reflections (R_{int})	4179(0.037)	4640(0.018)	3656(0.31)	3798(0.023)
R_1, wR_2 [$I>2\sigma(I)$]	0.0713, 0.1562	0.0423, 0.1193	0.0489, 0.1331	0.0478, 0.1036
R_1, wR_2 (all data)	0.1515, 0.1934	0.0571, 0.1289	0.0622, 0.1452	0.0768, 0.1204

Table 2 Geometry of the hydrogen bonds and short contacts

Compound	Interaction[a]	D ··· A/Å	D ··· H/Å	H ··· A/Å	<D-H ··· A/°
1·iso	N7–H7 ··· O2A	2.996(3)	0.96	2.04	174
	O1A–H1O ··· N1	2.603(3)	1.05(4)	1.55(3)	165(3)
	C5–H5 ··· O2A$^{(i)}$	3.761(3)	0.96	2.81	169
1·obe	N7–H7 ··· O2A	2.865(3)	0.96	1.92	169
	O1A–H1O ··· N1	2.646(3)	1.10(4)	1.55(4)	170(3)
	C5–H5 ··· O2A$^{(ii)}$	3.924(5)	0.96	2.98	167
1·oxa	N7–H7 ··· O2A	2.822(2)	0.96	1.86	178
	O1A ··· H1N ··· N1	2.678(2)	1.32(4)	1.36(3)	178(3)
	C5–H5 ··· O2A$^{(iii)}$	3.403(2)	0.96	2.45	171
1·seb	N7–H7 ··· O2A	2.955(2)	0.96	2.00	176
	O1A–H1O ··· N1	2.649(2)	0.99(4)	2.67(4)	172
	C5–H5 ··· O2A$^{(iv)}$	3.745(3)	0.96	2.79	175
1·sq	N7–H7 ··· O2A	2.734(5)	0.96	1.78	170
	N1–H1N ··· O1A	2.624(5)	1.00(5)	1.63(6)	171(5)
	C5–H5 ··· O2A$^{(iii)}$	3.251(6)	0.96	2.29	174
	C6–H6 ··· O1A$^{(v)}$	3.145(6)	0.96	2.38	139
	C9–H9 ··· O2A	3.249(6)	0.96	2.48	137
1·suc	N7–H7 ··· O2A	2.933(2)	0.96	1.97	177
	O1A–H1O ··· N1	2.647(2)	1.01(3)	1.66(3)	164(2)
	C5–H5 ··· O2A$^{(vi)}$	3.858(2)	0.96	2.90	178
	C6–H6 ··· O1A$^{(vii)}$	3.536(2)	0.96	2.60	166
1_2·tere	N7–H7 ··· O2A	2.832(2)	0.96	1.88	169
	N1–H1N ··· O1A	2.626(2)	0.98(2)	1.66(2)	171(2)
	N14–H14 ··· O1A$^{(viii)}$	2.882(2)	0.96	1.93	174
2·diph	N7–H7 ··· O2A	2.897(3)	0.96	1.95	167
	O1A–H1O ··· N1	2.590(3)	1.12(3)	1.53(3)	157(2)
	C5–H5 ··· O2A$^{(ix)}$	3.549(4)	0.96	2.67	153
2·mal	N7–H7 ··· O2A	2.774(2)	0.96	1.82	172
	N1–H1N ··· O1A	2.587(2)	1.12(3)	1.47(3)	172(3)
	C5–H5 ··· O2A$^{(x)}$	3.338(2)	0.96	2.61	164
2·seb	N7B–H7B ··· O2	2.945(3)	0.96	1.99	174
	O1–H1O ··· N1B	2.649(4)	0.99(5)	1.67(5)	169(4)
	C5B–H5B ··· O4$^{(xi)}$	3.523(4)	0.96	2.66	160
	N7A–H7A ··· O4	2.981(3)	0.96	2.03	171
	O3–H3O ··· N1A	2.616(4)	1.14(5)	1.49(5)	168(3)
	C5A–H5A ··· O2$^{(xIi)}$	3.580(5)	0.96	2.62	174
2·sq	N7–H7 ··· O2A	2.695(3)	0.96	1.75	167
	N1–H1N ··· O1A	2.604(3)	1.05(3)	1.59(3)	162(3)
	C5–H5 ··· O2A$^{(xii)}$	3.199(3)	0.96	2.27	163
	C6–H6 ··· O1A$^{(xiv)}$	3.227(3)	0.96	2.43	140
	C9–H9 ··· O2A$^{(i)}$	3.266(3)	0.96	2.48	139
2·tere	N7–H7 ··· O2A	2.863(2)	0.96	1.91	172
	N1–H1N ··· O1A	2.544(2)	1.16(3)	1.41(3)	164(3)
	C5–H5 ··· O2A$^{(xv)}$	3.509(2)	0.96	2.59	161
	C10–H10 ··· O1A$^{(xvi)}$	3.440(2)	0.96	2.56	152
	C9–H9 ··· O1A$^{(xvii)}$	3.337(2)	0.96	2.41	162
3_2·tere·$(EtOH)_2$	N7–H7 ··· O2A	2.847(3)	0.96	1.89	174
	N1–H1N ··· O1A	2.534(4)	1.09(4)	1.45(4)	170(3)
	C5–H5 ··· O2A$^{(i)}$	3.551(5)	0.96	2.65	156
	N21–H21 ··· N23$^{(xviii)}$	2.987(7)	0.96	2.06	162
	O1E–H1E ··· O1A$^{(xv)}$	2.782(4)	0.96	1.84	165
4·tere·H_2O	N7–H7 ··· O2A	2.802(2)	0.96	1.81	175
	N1–H1N ··· O1A	2.648(2)	1.01(2)	1.64(2)	176(2)
	N21–H21 ··· O4A$^{(xix)}$	2.766(2)	0.96	1.80	178
	N23–H23 ··· O3A$^{(xix)}$	2.599(2)	1.17(2)	1.43(2)	176(2)
	O1W–H1WA ··· O2A$^{(xx)}$	2.956(2)	0.96	2.02	168
	O1W–H1WB ··· O2A	2.911(2)	0.96	1.96	175
	C9–H9 ··· O4A$^{(xxi)}$	3.502(2)	0.96	2.57	165
	C10–H10 ··· O4A$^{(xxii)}$	3.583(2)	0.96	2.63	162
	C17–H17 ··· O4A$^{(xx)}$	3.343(2)	0.96	2.55	142
5_2·fum	N7–H7 ··· O2A	2.886(2)	0.96	1.93	176
	N1–H1N ··· O1A	2.563(2)	1.19(3)	1.39(3)	168(2)
	N21–H21 ··· O2A	3.263(3)	0.96	2.31	173
	C24–H24 ··· O1A$^{(xiv)}$	3.578(3)	0.96	2.80	138
	C2′A–H2A ··· N23$^{(xiv)}$	3.473(6)	0.96	2.55	163
5_2·tere	N7–H7 ··· O2A	2.933(2)	0.96	1.99	169
	N1–H1N ··· O1A	2.545(2)	1.25(2)	1.31(2)	170(2)
	N21–H21 ··· O2A	3.172(2)	0.96	2.22	170
	C5–H5 ··· O2A$^{(viii)}$	3.456(3)	0.96	2.64	142
	C3A–H3A ··· N23	3.451(3)	0.96	2.54	160

[a] Symmetry codes: (i) 1 + x,y,z; (ii) x,1 + y,z; (iii) x,y,1 + z; (iv) x − 1,y,z + 1; (v) − x,1 − y,2 − z; (vi) 1 + x,y,z + 1; (vii) 1 − x,1 − y, − z; (viii) x − 1,y,z; (ix) x − 1,y,z; (x) 0.5 + x,y − 0.5,z; (xi) 1 − x, − y, − 1 − z; (xii) 3 − x, − 1 − y, − 1 − z; (xiii) 1 + x, y − 1,z; (xiv) − x,1 − y, − z; (xv) x,y − 1,z; (xvi) 1 − x, − y,2 − z; (xvii) − x, − y,2 − z; (xviii)1 − x, − 1 − y, − z; (xix) x + 1,y − 1,z + 1; (xx)1 − x,1 − y,1 − z; (xxi) − x,1 − y,1 − z; (xxii) x,y − 1,z + 1.

the values of the CNC bond angle within the pyridine unit remain in the range of 118.3–119.2°. The latter geometric parameter is known as a useful indicator of the protonation state of the pyridine nitrogen.[12] For comparison these values in *N*,*N*′-bis(2-pyridyl)aryldiamines **1**–**4**, characterized by relatively weak N–H ··· N interactions, fall in the range of 116.6–117.9°, with the mean value of 117.2°.[5]

In the case of the complexes $\mathbf{1}_2$**·tere**, **2·tere**,$\mathbf{3}_2$**·tere·(EtOH)$_2$**, **1·sq** and **2·sq** the X-ray data point to a proton transfer from both carboxylic groups to the pyridine nitrogens. However, in the 2 : 1 complexes: $\mathbf{1}_2$**·tere** and $\mathbf{3}_2$**·tere·(EtOH)$_2$**, only one pyridine nitrogen is protonated. The corresponding N–H distances in the protonated pyridine moieties fall in the range of 0.98–1.16 Å and the CNC angles in the range of 121.4–122.6°. The two carboxylate C–O bond lengths differ only by 0.4 Å and the higher value corresponds to the oxygen involved in the strong charge-assisted N^+–H ··· O^- interaction. In **4·tere·H$_2$O**, a complete proton transfer from one carboxylic group to the pyridine nitrogen is observed (N–H 1.01 Å, CNC 122.1°) whereas the geometric parameters indicate only a partial deprotonation of the second carboxylic group (N–H 1.17 Å, CNC 120.1°).

The crystallographic data for the remaining complexes are not conclusive in respect to their protonation state, even though the carboxylic hydrogens can be found on the difference Fourier maps. In **2·mal**, $\mathbf{5}_2$**·fum** and $\mathbf{5}_2$**·tere** they are located closer to the pyridine nitrogens than to the carboxylic oxygens whereas in **1·oxa** the hydrogen was found nearly at the middle of the NH ··· O bridge (see Table 2). The pyridine CNC angles of 119.5–120.5° also point to an intermediate state in which the pyridine moiety is neither fully protonated nor neutral. This might be due to the proton disorder over two positions in the NH ··· O bridge. In effect, the same site in the crystal is occupied by a pyridinium cation and a neutral pyridine moiety, *i.e.* the dicarboxylic acid is only partially deprotonated.

To summarize, the studied 1 : 1 complexes of *N*,*N*′-bis-(2-pyridyl)aryldiamine with dibasic acids can be grouped into (a) neutral complexes B·H_2A, (b) ionic salts BH_2^{+2}·A^{-2} with a complete transfer of the two protons from the acid to the base and (c) ionic salts BH_x^{+x}·$A^{-(2-x)}$ with only partial transfer of protons from the acid to the base.

The crystal structures of the sixteen studied complexes reveal that the recognition between the carboxylic acids and the 2-aminopyridine units occurs through the formation of the cyclic hydrogen bond $R^2_2(8)$ motifs **IIa** or **IIb**, whereas squaric acid generates the analogous $R^2_2(8)$ motif **IIIb** with the graph symbol $R^2_2(9)$. Both carboxylic acids and 2-aminopyridines comprise self-complementary functional groups defined by H-bond donor-acceptor pairs and therefore can potentially interact via homomeric $R^2_2(8)$ ring motifs. However, the CSD search[4c] shows that the probability of generation of motif **I** (26%) or carboxylic acid dimer (37%) is much lower than the probability of formation of the motifs **IIa** or **IIb** (76 and 82%, respectively) and therefore the synthons **IIa,b** belong to the most powerful tools used in crystal engineering. Among the studied complexes the homomeric dimer of 2-aminopyridine units was observed only once, in the 2 : 1 complex $\mathbf{3}_2$**·tere·EtOH$_2$** where double deprotonation of the terephthalic acid resulted in its loosing complementarity with the neutral 2-aminopyridine moiety of **3**.

The self-assembly patterns observed in the crystal structures of the 1 : 1 complexes of **1** are presented in Figs 1–4. The complexation with use of the hydrogen bond motifs **IIa,b** or **IIIa,b** in the case of dicarboxylic acids and squaric acid, respectively, results in the formation of 1D networks with alternating component molecules (see Scheme 1). In **1·suc**, **1·seb**, **1·oxa**, *i.e.* in the co-crystals formed by **1** with centrosymmetric dicarboxylic acids, and in **1·sq**, where squaric acid exists as a centrosymmetric squarate dianion, the 1D networks belong to the rod group symmetry[13] $P2_1/m$ with component molecules (neutral or ionic) occupying special positions. The translational parameter of the 1D network depends on the length of the spacer joining the two carboxylic groups. The values of the unit-cell *b* parameters for **1·oxa**, **1·suc** and **1·seb** (Table 1) point to *ca.* 2.6 Å increase of this parameter for every CH_2–CH_2– unit added to the spacer. Because all proton donors of the molecular components of the complex are employed in the construction of the 1D networks, further organization of the crystal structures can be rationalized from the point of view of the close-packing principle.[16] In all complexes of **1** with the 1 : 1 stoichiometry, the acid–base chains related by unit translation of *ca.* 9 Å in a direction perpendicular to the 1D network form densely packed layers with the molecules of **1** in close contacts with two neighboring bis-pyridylamine molecules located on the same mirror plane (Fig. 5). This arrangement in all co-crystals leads to a repeating nearly linear C5–H ··· O2A interaction between pyridine H5 atoms and carboxylic O2A that belong to two adjacent 1D networks. The H5 ··· O2A distances range between 2.29 and 2.98 Å with the smallest values observed for **1·oxa** and **1·sq** (Table 2). The corrugated layers formed by close-packing of the hydrogen-bonded 1D networks are shown in Figs 1–4. Their symmetry depends on the symmetry of the site occupied by the acid molecule. For the complexes shown in Figs 1 and 2, where the acid molecule is situated at the inversion center, the layers belong to the $P2_1/m$ layer group symmetry.[13] In **1·suc** and **1·seb** these layers stack by monoclinic translation building the crystal in the space group $P2_1/m$. In the two isostructural complexes, **1·oxa** and **1·sq**, the neighboring layers are related by the 2_1 axis perpendicular to the layer giving rise to the

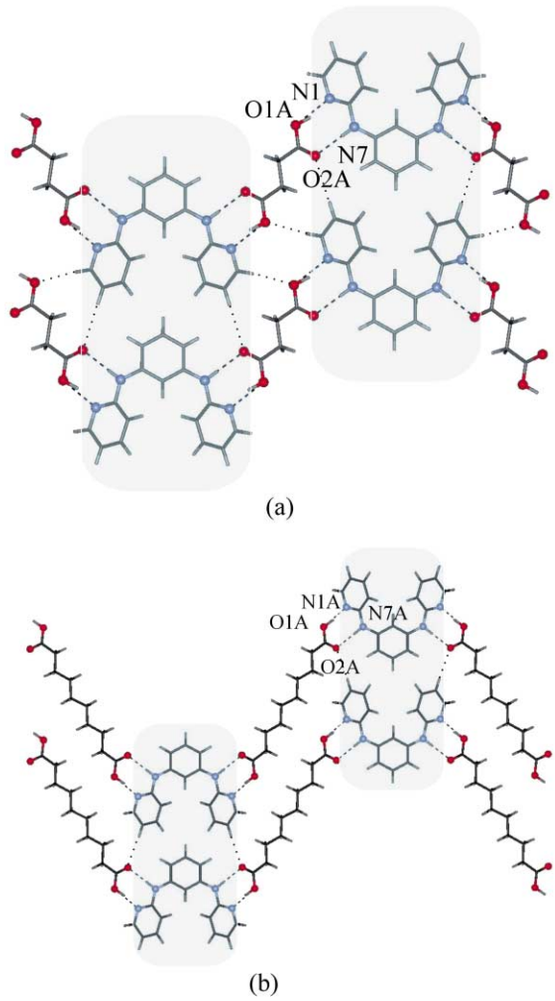

Fig. 1 1D networks and close-packed layers in the crystal structure of **1·suc** (a) and **1·seb** (b). Spheres represent N and O atoms. Hydrogen bonds are drawn with dashed lines. The shaded areas indicate close-packed chains of **1**.

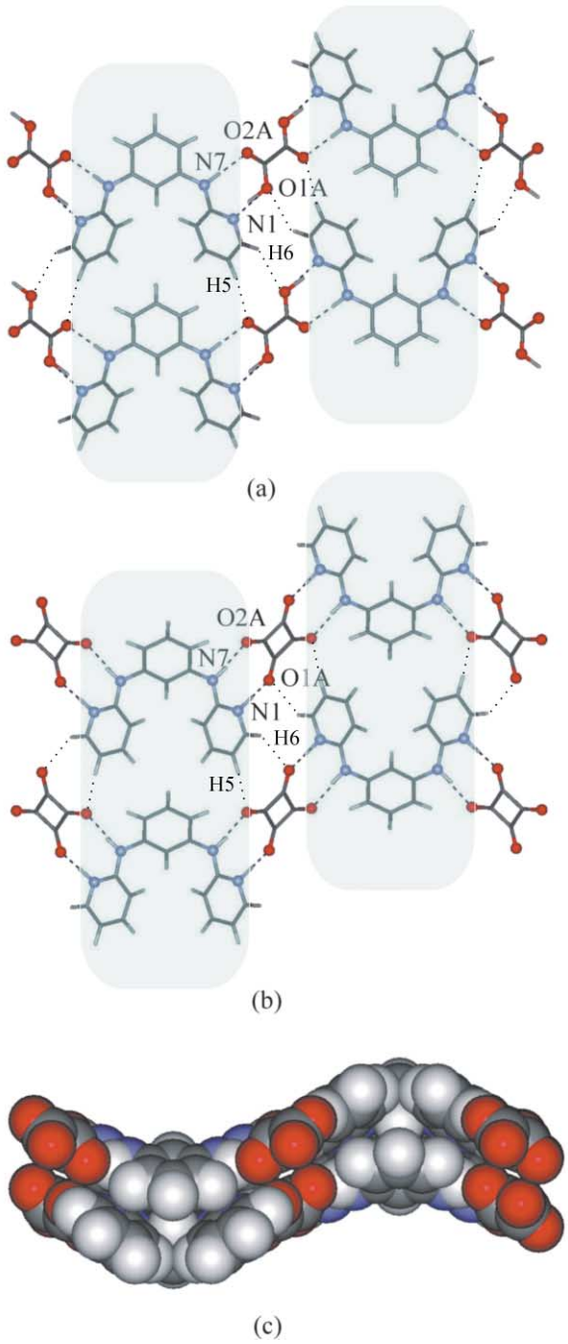

Fig. 2 1D networks and close-packed layers in the isostructural complexes **1·oxa** (a) and **1·sq** (b) and side view of the corrugated layer in **1·sq** (c).

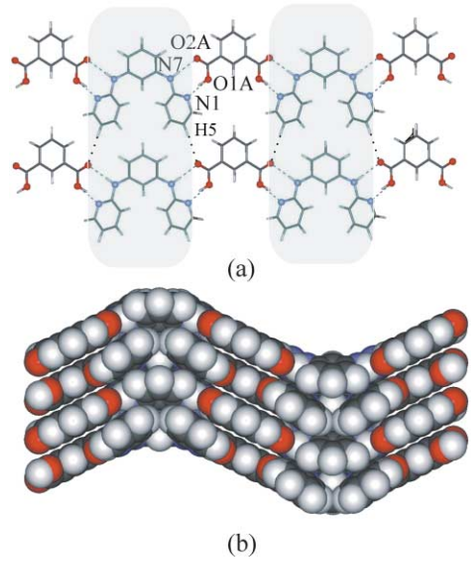

Fig. 3 1D network and polar close-packed layer in the crystal structure of **1·iso:** (a) top view of the layer; (b) side view of the stacked layers. The polarity direction is parallel to the layer.

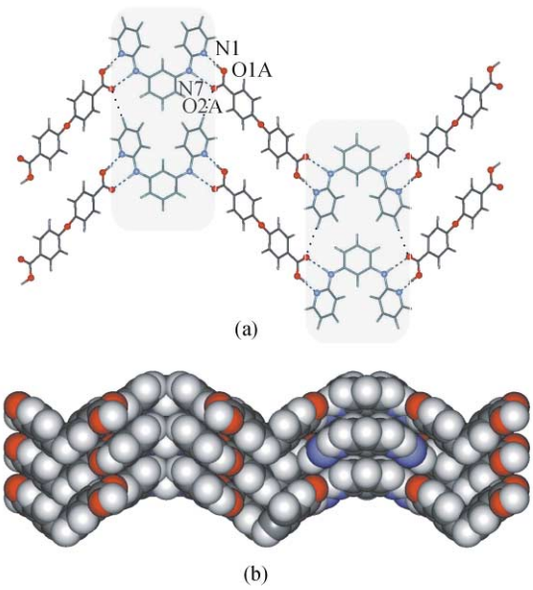

Fig. 4 1D network and polar close-packed layer in the crystal structure of **1·obe:** (a) top view of the layer; (b) side view of the stacked layers. The polarity direction is perpendicular to the layer.

crystal orthorhombic *P* nma space group. In the remaining 1 : 1 complexes of **1**, shown in Figs 3 and 4, the dicarboxylic acid molecules reside on 2-fold axes and therefore the resulting hydrogen-bonded 1D network (rod group *P*ma2) and close-packed layers are polar. However, in **1·iso** anti-parallel stacking of the layers leads to a centrosymmetric crystal. In turn, in **1·obe**, where the polarity axis is perpendicular to the close-packed layer, parallel stacking of the layers produces a polar crystal.

The persistent formation of hydrogen-bonded 1D networks generated by the motifs **IIa,IIb**, or **IIIa,b**, in ionic or molecular complexes of the title compounds is further illustrated by the crystal structures of the 1:1 complexes of **2** (Figs 6–8). The infinite zig-zag tapes formed via assembly of **2** with the squaric, terephthalic and sebacic acids reveal the $P\bar{1}$ rod group symmetry (Fig. 6). Analogously to the packing mode observed in the co-crystals of **1**, the hydrogen-bonded 1D networks are further organized *via* translation of *ca.* 9 Å into densely packed layers in which each molecule of **2** is in close contact with two neighbors forming several short intermolecular hydrogen ··· hydrogen contacts (Fig. 9). The edge-to-face stacking interactions between pyridine and benzene rings provide, most likely, some additional stabilization energy to the chain arrangement shown in Fig. 9. The densely packed layers are nearly flat, with the 2-aminopyridine and acid units located approximately in one plane and the central benzene ring of **2** strongly twisted relative to the linked 2-aminopyridine moieties, sticking on both sides of the layer. Again a nearly linear C5–H ··· O2A interaction between the pyridine H5 atoms and the carboxylic O2A atoms is repeated in all complexes of **2**. The H5 ··· O2A distances are in the range of 2.27–2.67 Å with the shortest value observed in the squarate complex **2·sq** (Table 2).

As illustrated by the crystal structures of **2·mal** and **2·diph** (Figs 7 and 8) the close-packed layers are no longer flat in these complexes. They are strongly folded but there are some flat areas involving planar carboxylic (**2·mal**) or 4-phenylcarboxylic groups (**2·diph**).

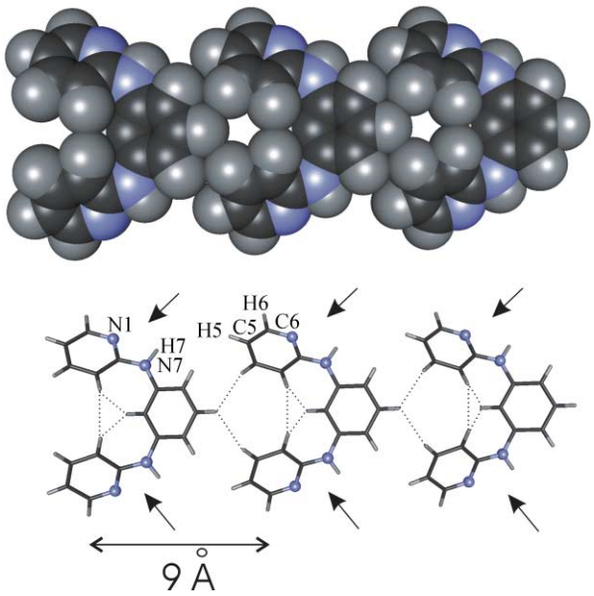

Fig. 5 The close-packed chain of molecules of **1** observed in all 1:1 complexes of **1** with dibasic acids (autostereogram[14]). Dotted lines indicate the shortest intramolecular and intermolecular H ··· H contacts in the chain. Arrows show the sites of carboxylic group recognition.

In the **4·tere·H_2O** adduct dicarboxylic acid and bis-pyridylamine molecules are connected into 1D network analogous to that observed in the 1 : 1 complexes of **1** and **2**. Water molecules included during crystallization are used as 'clips' connecting two neighboring acid–base 1D networks into larger hydrogen bonded 1D aggregates (Fig. 10). The oxygen atom O2A of one of the carboxylate groups accepts two hydrogen bonds from water molecules whereas the second carboxylate group acts as an acceptor in the shortest C–H ··· O interactions in the crystal (Table 2).

The $R^2_2(8)$ rings are again principle motifs in the 1D network observed in the complex **3_2·tere·$(EtOH)_2$**. The monoprotonated molecules of **3** form dimers *via* the self-complementary interactions **I** between non-protonated 2-aminopyridine units and the protonated units and are connected *via* the complementary interactions **IIb** to the terephthalic dianions located at inversion center. Fig. 11 shows two such 1D networks related by the unit translation of 8.783 Å along the *x* axis. It can be easily noticed that the fragment comprising terephthalic dianions and the protonated halves of **3** resemble a closely analogous fragment in the structure of **2·tere** (Fig. 6b) with the same set of the short intermolecular contacts. The ethanol molecules are joined *via* O–H ··· O interactions to the carboxylate groups approaching them from below and above the plane defined by the protonated 2-aminopyridine units and the terephthalic anions and fill the voids created between the neighboring chains.

The remaining 2 : 1 adducts have completely different structures. In the case of **1_2·tere** the monoprotonated molecules of **1** and the terephthalic dianions (Fig. 12) create, *via* hydrogen bonds, a ladder-type 1D network. The molecules of **1** assume the (*E,Z*)-conformation and the protonated 2-aminopyridine units in the (*E*)-conformation bind to the carboxylic anions generating the motif **IIb**. The amino hydrogen of the second 2-aminopyridine unit, adopting the (*Z*)-conformation, participates in hydrogen bonding to the carboxylate oxygen O1A. The aminopyridine unit in the (*Z*)-conformation is only slightly tilted to the central benzene ring while the second group is nearly perpendicular [the corresponding dihedral angles are 16.2(1) and 89.2(1)°, respectively].

The crystal structure of **1_2·tere**, where each carboxylic group is hydrogen bonded to two 2-aminopyridine units could lead to the idea of constructing a tritopic receptor based on the bis-pyridylamine system, which could efficiently recognize

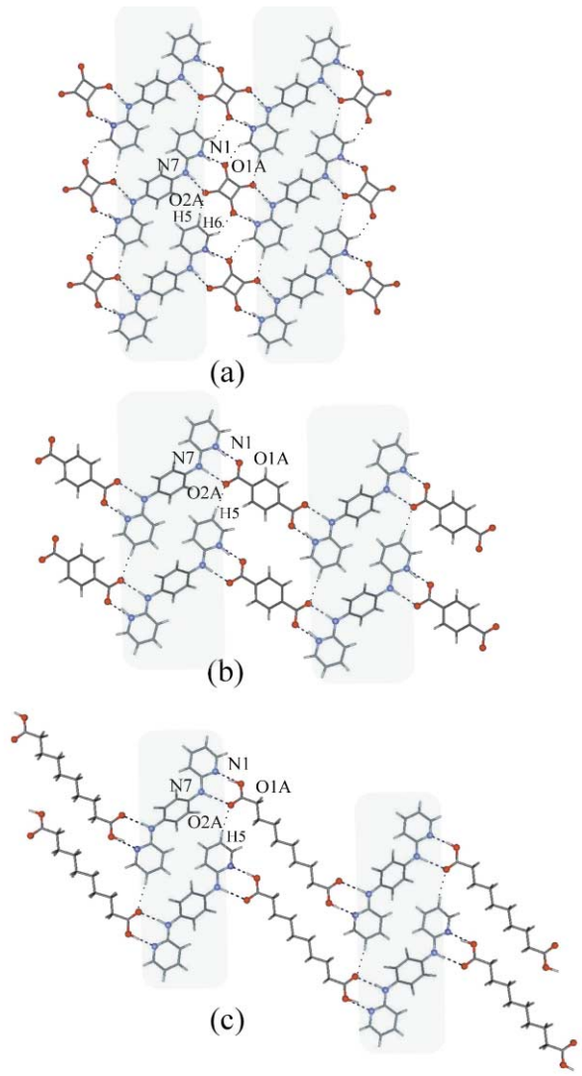

Fig. 6 1D networks and close-packed layers in the crystal structure of (a) **2·sq**, (b) **2·tere** and (c) **2·seb** (b). Spheres represent N and O atoms. Hydrogen bonds are drawn with dashed lines. The shaded areas indicate close-packed chains of **2**.

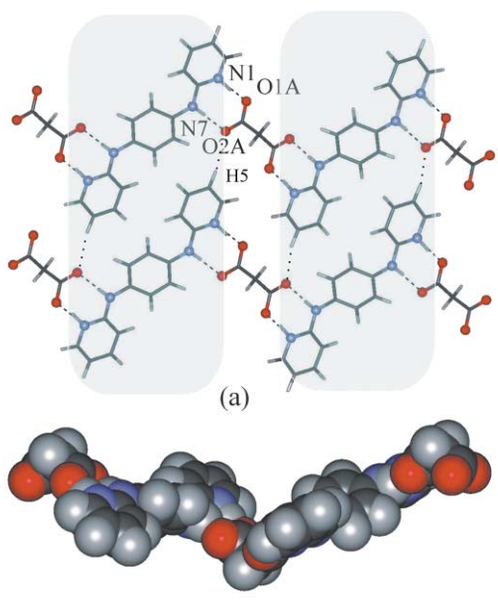

Fig. 7 1D network and close-packed layer in the crystal structure of **2·mal**: (a) top view of the layer; (b) side view of the layers.

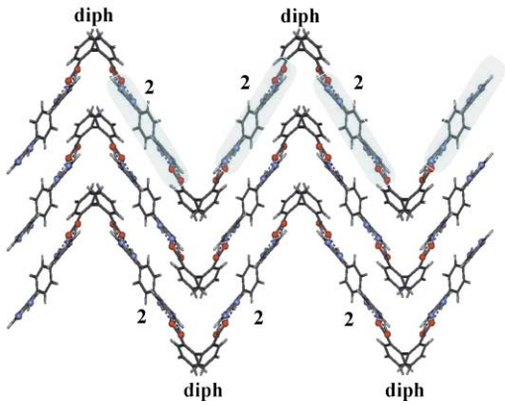

Fig. 8 Side view of the stacking of strongly corrugated layers composed of densely packed, hydrogen-bonded 1D networks in the crystal structure of **2·diph**. Chains of **2**, shown by the shaded areas, run perpendicular to the plane of the drawing.

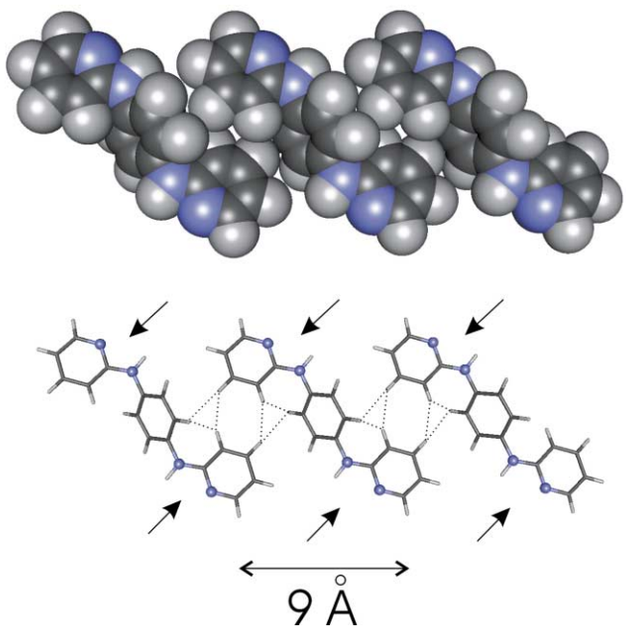

Fig. 9 The close-packed chain of the molecules of **2** observed in all 1 : 1 complexes of **2** with diacids (autostereogram[14]). Dotted lines indicate the shortest intramolecular and intermolecular hydrogen ··· hydrogen contacts in the chain. Arrows show the sites of carboxylic group recognition.

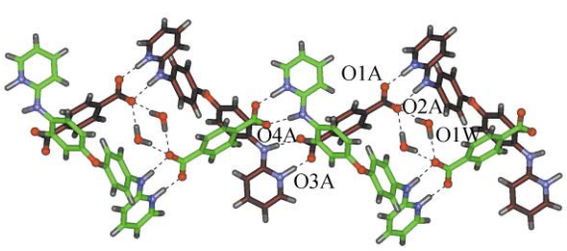

Fig. 10 Hydrogen-bonded 1D aggregates composed of two 1D acid-base networks connected *via* water molecules in the crystal structure of **4·tere·H_2O**. The two acid–base 1D networks are distinguished by different colors.

carboxylic acids as well as carboxylate anions. Thus we synthesized the *N*, *N′*-bis(2-pyridyl)aryldiamine **5** with two 2-aminopyridine units positioned in a manner which makes it possible to bind the carboxyl *via* three hydrogen bonds. Since both 2-aminopyridine units are involved in coordination of one carboxylic group, the complexes formed by **5** with dicarboxylic acids should have predominantly 2 : 1 molecular stoichiometry and should generate discrete hydrogen-bonded assemblies.

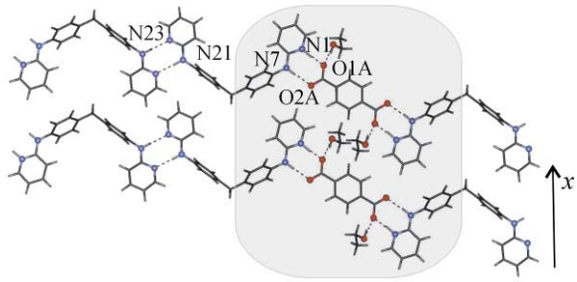

Fig. 11 Hydrogen bonded 1D networks formed *via* alternating motifs **I** and **II** in the crystal structure of **3_2·tere·$(EtOH)_2$**.

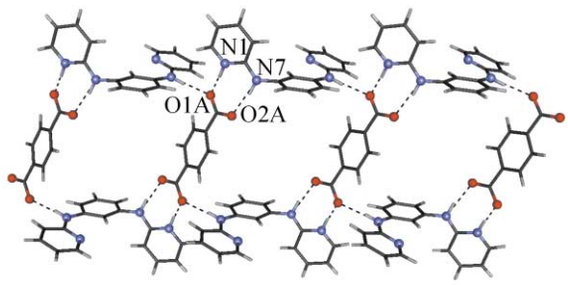

Fig. 12 Hydrogen bonded 1D network in the crystal structure of **1_2·tere** [notice (*E,Z*) conformation of **1**] (autostereogram[15]).

Indeed, the crystal structures of the co-crystals **5_2·tere** and **5_2·fum** showed that the dicarboxylic acid molecules bind to two molecules of **5** through six N–H ··· O hydrogen bonds creating the centrosymmetric discrete assemblies presented in Fig. 13. Whereas formation of the heteromeric $R^2_2(8)$ motif **II** forces one of two 2-aminopyridine units to adopt the (*E*)-conformation, the second one can assume either the (*Z*) or

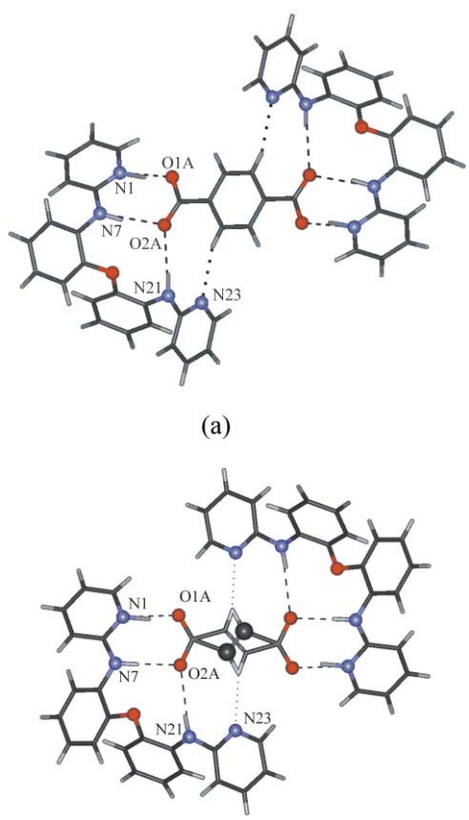

Fig. 13 Discrete hydrogen-bonded assemblies of dicarboxylic acid and and **5** in the crystal structures of (a) **5_2·tere** and (b) **5_2·fum**; the fumaric acid is disordered over two positions. Spheres represent N and O atoms. Hydrogen bonds are drawn with dashed lines.

(*E*) geometry, however, due to the stabilizing C–H ··· N interactions, adopts the (*E*)-conformation. The fumaric acid molecule in **5_2·fum** is disordered over two sites, yet the disorder has no influence on its hydrogen-bonding mode.

In conclusion, we have shown that co-crystallization of *N*,*N*′-bis(2-pyridyl)aryldiamines with a variety of dibasic acids including aliphatic and aromatic dicarboxylic acids as well as squaric acid results in formation of the 1 : 1 complexes, which depending of the acid strength, can be either neutral or ionic. By combining the two components it is possible to create predictable supramolecular structures of alternating components assembled into infinite tapes. Though the 2-aminopyridine and carboxylic acid moieties are known to form homomeric dimers, our results provide further confirmation that they prefer interacting with each other creating $R^2_2(8)$ the motifs. The dicarboxylic acid sub-units can be replaced by the squaric acid molecules giving rise to analogous tightly bonded tape structures controlled by the $R^2_2(9)$ cyclic hydrogen bonds.

Experimental

The synthesis of compounds **1**–**4** has been described earlier.[5] Dicarboxylic acids and squaric acid were purchased from Aldrich and used without purification. ^{1}H and ^{13}C NMR spectra were obtained with Bruker DRX-500 and WP-200 spectrometers at 500 and 50 MHz, respectively. The deuteriated solvents were used as an internal lock for ^{1}H and ^{13}C NMR. FT-IR absorptions were taken with a Bruker IFS66 spectrometer.

Syntheses

***N*,*N*′-Bis(2-pyridyl)-2,2′-oxybis(aminobenzene) (5).** 2,2′-Oxybisaniline[16] (1.00 g, 5 mmol) was dissolved in 2-chloropyridine (2.8 ml, 30 mmol) and refluxed for *ca.* 30 min. After cooling the reaction mixture was diluted with benzene (5 ml) and extracted with water to separate the hydrochloride. The aqueous layer was treated with 25% aqueous ammonia (10 ml) and extracted with benzene. The organic layer was dried (Na_2SO_4), evaporated to dryness and the residue was recrystallized from benzene. The product crystallizes with one molecule of benzene, yield 1.65 g (76%): mp 120–122 °C; δ_H ($CDCl_3$) 8.23 (d, J = 4.9 Hz, 2H), 8.17 (d, J = 8.2 Hz, 2H), 7.52 (m, 2H), 7.38(s, 6H, C_6H_6), 7.19 (br s, 2H, NH), 7.14 (t, J = 7.7 Hz, 2H), 6.94 (t, J = 7.0 Hz, 2H), 6.91 (t, J = 8.0 Hz, 2H), 6.83 (d, J = 8.5 Hz, 2H) and 6.77 (m, 2H); δ_C ($CDCl_3$) 155.3, 147.8, 146.0, 137.4, 132.0, 128.3 (C_6H_6), 124.1, 122.2, 120.0, 118.0, 115.2 and 110.0; ν_{max}(KBr)/ cm^{-1} 3419, 3279, 3220, 1606, 1521 and 11483. Anal. calcd for $C_{22}H_{18}N_4O{\cdot}C_6H_6$ (432.53): C, 77.75; H, 5.59; N, 12.95; found: C, 77.36; H, 5.61; N, 12.97.

Preparation of the *N*,*N*′-bis(2-pyridyl)aryldiamine co-crystals. Equimolar amounts of the *N*,*N* ′-bis(2-pyridyl)aryldiamines and dicarboxylic acids were dissolved in boiling ethanol and allowed to crystallize slowly at room temperature. In the case of the squaric acid complexes the aqueous solution of the acid was added to the *N*,*N* ′-bis(2-pyridyl)aryldiamine in hot ethanol and the mixture was left to stand at room temperature. The resulting co-crystals were removed from the solution before the solvent had completely evaporated.

***N*,*N*′-Bis(2-pyridyl)-1,3-diaminobenzene–1,3-benzenedicarboxylic acid co-crystal (1·iso).** Colorless bricks, mp 211–212 °C; λ_{max}(KBr)/cm^{-1} 3260, 3201, 2350 (br), 1860 (br), 1678, 1608, 1576, and 1436.

***N*,*N*′-Bis(2-pyridyl)-1,3-diaminobenzene–oxalic acid co-crystal (1·oxa).** Colorless needles, mp 198–199 °C; λ_{max}(KBr)/ cm^{-1} 3255, 3201, 2630 (br), 1905 (br), 1678, 1680, 1645, 1610, 1577, 1433 and 1234.

***N*,*N*′-Bis(2-pyridyl)-1,3-diaminobenzene–succinic acid co-crystal (1·suc).** Colorless bricks, mp 187–188 °C; λ_{max}(KBr)/ cm^{-1} 3271, 3208, 2400 (br), 1900 (br), 1692, 1603, 1577 and 1439.

***N*,*N*′-Bis(2-pyridyl)-1,3-diaminobenzene–sebacic acid co-crystal (1·seb).** Colorless bricks, mp 138 °C; λ_{max}(KBr)/cm^{-1} 3271, 3207, 2410 (br), 1890 (br), 1694, 1601, 1577 and 1433.

***N*,*N*′-Bis(2-pyridyl)-1,3-diaminobenzene–4,4′-oxybis-benzoic acid co-crystal (1·obe).** Colorless prisms, mp 158–200 °C; λ_{max}(KBr)/cm^{-1} 3256, 3176, 2450 (br), 1850 (br), 1612, 1596, 1484 and 1450.

***N*,*N*′-Bis(2-pyridyl)-1,3-diaminobenzene–1,4-benzenedicarboxylic acid co-crystal (1_2·tere).** Yellow bricks, mp 210–212 °C; λ_{max}(KBr)/cm^{-1} 3292, 3191, 2850 (br), 2460 (br), 1900 (br), 1676, 1627, 1589, 1537, 1484 and 1378.

***N*,*N*′-Bis(2-pyridyl)-1,3-diaminobenzene–squaric acid co-crystal (1·sq).** Fine yellow needles, mp 287–288 °C (with decomp.); λ_{max}(KBr)/ cm^{-1} 2585 (br), 1890 (br), 1980, 1629, 1580, 1510 and 1473.

***N*,*N*′-Bis(2-pyridyl)-1,4-diaminobenzene–1,4-benzenedicarboxylic acid co-crystal (2·tere).** Thin plates, begins to melt at 259 °C; λ_{max}(KBr)/cm^{-1} 3268, 2850 (br), 1940 (br), 1615, 1519, 1441 and 1349.

***N*,*N*′-Bis(2-pyridyl)-1,4-diaminobenzene–malonic acid co-crystal (2·mal).** Fine needles, mp 198–199 °C (with decomp.); λ_{max}(KBr)/cm^{-1} 3267, 2850 (br), 2520 (br).1990 (br), 1737, 1667, 1625, 1373, and 1340.

***N*,*N*′-Bis(2-pyridyl)-1,4-diaminobenzene–sebacic acid co-crystal (2·seb).** Thin plates, mp 185–186 °C; λ_{max}(KBr)/cm^{-1} 3258, 3178, 2415 (br), 1900 (br), 1689, 1607, 1586 and 1441.

***N*,*N*′-Bis(2-pyridyl)-1,4-diaminobenzene–2,2′-biphenyldicarboxylic acid co-crystal (2·diph).** Colourless blocks, mp 216 °C; λ_{max}(KBr)/cm^{-1} 3260, 3180, 2390 (br), 1900 (br), 1661, 1594, 1515 and 1444.

***N*,*N*′-Bis(2-pyridyl)-1,4-diaminobenzene–squaric acid co-crystal (2·sq).** Fine yellow needles, mp 284–285 °C (with decomp.); λ_{max}(KBr)/cm^{-1} 2585 (br), 1990 (br), 1630, 1540, 1490 and 1426.

***N*,*N*′-Bis(2-pyridyl)-4,4′-methylenebis(aminobenzene)–1,4-benzenedicarboxylic acid co-crystal [3_2·tere·($EtOH)_2$].** Colourless prisms, clouds at 76 °C and begins to melt at 176 °C; λ_{max}(KBr)/ cm^{-1} 3429, 3164, 2920 (br), 1950 (br), 1689, 1597, 1527, 1506, 1437, 1355 and 1330.

***N*,*N*′-Bis(2-pyridyl)-4,4′-oxybis(aminobenzene)–1,4-benzenedicarboxylic acid co-crystal (4·tere·H_2O).** Colourless prisms, begins to melt at 176 °C; λ_{max}(KBr)/ cm^{-1} 3244, 2900 (br), 2420 (br), 1910 (br), 1677, 1641, 1501 and 1439.

***N*,*N*′-Bis(2-pyridyl)-2,2′-oxybis(aminobenzene)–fumaric acid co-crystal (5_2·fum).** Colourless bricks, mp 160–161 °C; λ_{max}(KBr)/ cm^{-1} 3341, 3257, 2860 (br), 2500 (br), 1950 (br), 1608, 1588, 1520, 1448 and 1252.

***N*,*N*′-Bis(2-pyridyl)-2,2′-oxybis(aminobenzene)–1,4-benzenedicarboxylic acid co-crystal (5_2·tere).** Colourless bricks begins to melt at 150 °C; λ_{max}(KBr)/ cm^{-1} 3310, 2850 (br), 2450 (br), 1671, 1611, 1590, 1512 and 1447.

X-Ray diffraction analysis ‡

X-Ray diffraction studies were carried out using a Kuma Diffraction KM-4 diffractometer for **1·oxa**, **1·suc**, **2·diph**, **2·mal and 2·tere** and Kuma CCD diffractometer for the remaining co-crystals. The data were collected at room temperature except for **1·obe**, **1·seb**, **1·sq and 2·sq** (100 or 130 K) and were corrected for Lorentz and polarization factors; absorption correction was not applied. The structures were solved by direct methods using SHELXS-97[17] and refined by the full-matrix least-squares method using the SHELXL-97 program.[18] The CH hydrogen atoms were placed geometrically and they were allowed to ride on the pivot atom; their isotropic displacement parameters were refined. The amino group hydrogen atoms were located on the ΔF maps and the N–H distances standardized to 0.96 Å. They were allowed to ride on the pivot atom; their isotropic displacement parameters were refined. The NH and OH hydrogen atoms were located on the ΔF maps and their positional and isotropic displacement parameters included in the refinement. In $\mathbf{5_2}$**·fum** the fumaric acid molecule is disordered over two positions with nearly equal occupancies.

‡ CCDC reference numbers 191434–191449. See http://www.rsc.org/suppdata/ob/b2/b211675h/ for crystallographic data in .cif or other electronic format.

Acknowledgements

Financial support from the Committee of Scientific Research (project no. 3 T09 098 18) is gratefully acknowledged.

References

1 (*a*) G. R. Desiraju, *Crystal Engineering: The Design of Organic Solids*, Elsevier, Amsterdam, 1989; (*b*) *The Crystal as a Supramolecular Entity*, ed. G. R. Desiraju, Wiley, Chichester, 1995; (*c*) *Organic Molecular Solids. Properties and Applications*, ed. W. Jones, CRC Press, Boca Raton, 1997; (*d*) D. N. Chin, J. A. Zerkowski, J. C. MacDonald and G. M. Whitesides, in *Organised Molecular Assemblies in the Solid State*, ed. J. K. Whitesell, Wiley, Chichester, 1999, ch. 5; (*e*) B. Moulton and M. J. Zaworotko, *Chem. Rev.*, 2001, **101**, 1629.

2 J.-M. Lehn, *Supramolecular Chemistry: Concepts and Perspectives*, VCH, Weinheim, 1995.

3 (*a*) J. C. MacDonald and G. M. Whitesides, *Chem. Rev.*, 1994, **94**, 2383; (*b*) D. Su, X. Wang, M. Simard and J. D. Wuest, *Supramol. Chem.*, 1995, **6**, 171; (*c*) J. R. Fredericks and A. D. Hamilton, in *Comprehensive Supramolecular Chemistry*, vol. 9, ed. J. L. Atwood, J. E. D. Davis, D. D. MacNicol and F. Vögtle, Pergamon, Oxford, 1996, ch. 16; (*d*) S. Coe, J. J. Kane, T. L. Nguyen, L. M. Toledo, E. Wininger, F. W. Fowler and J. W. Lauher, *J. Am. Chem. Soc.*, 1997, **119**, 86; (*e*) R. E. Melendez and A. D. Hamilton, *Top. Curr. Chem.*, 1998, **198**, 97.

4 (*a*) G. R. Desiraju, *Angew. Chem., Int. Ed.*, 1995, **34**, 2311; (*b*) G. R. Desiraju, *Chem. Commun.*, 1997, 1475; (*c*) A. Nangia and G. R. Desiraju, *Top. Curr. Chem.*, 1998, **198**, 57; (*d*) F. H. Allen, W. D. S. Motherwell, P. R. Rainthby, G. P. Shields and R. Taylor, *New. J. Chem.*, 1999, **23**, 25.

5 Part I: I. Bensemann, M. Gdaniec and T. Poloński, *New. J. Chem.*, 2002, **26**, 448.

6 For details of the definition, terminology, and notation in the graph set approach, see: (*a*) M. C. Etter, *Acc. Chem. Res.*, 1990, **23**, 120; (*b*) J. Bernstein, R. E. Davis, L. Shimoni and N.-L. Chang, *Angew. Chem., Int. Ed. Engl.*, 1995, **34**, 1555.

7 (*a*) M. C. Etter, Z. Urbańczyk-Lipkowska, M. Zia-Ebrahimi and T. W. Panunto, *J. Am. Chem. Soc.*, 1990, **112**, 8415; (*b*) M. C. Etter and S. M. Reutzel, *J. Am. Chem. Soc.*, 1991, **113**, 2586; (*c*) S. Hanessian, M. Simard and S. Roelens, *J. Am. Chem. Soc.*, 1995, **117**, 7680; (*d*) V. R. Pedireddi, S. Chatterjee, A. Ranganathan and C. N. R. Rao, *Tetrahedron*, 1998, **54**, 9457; (*e*) A. Ranganathan, V. R. Pedireddi and C. N. R. Rao, *J. Am. Chem. Soc.*, 1999, **121**, 1752.

8 (*a*) F. Garcia-Tellado, S. J. Geib, S. Goswami and A. D. Hamilton, *J. Am. Chem. Soc.*, 1991, **113**, 9265; (*b*) J. Geib, C. Vincent, E. Fan and A. D. Hamilton, *Angew. Chem., Int. Ed. Engl.*, 1993, **32**, 119; (*c*) E. Fan, J. Yang, J. Geib, T. C. Stoner, M. D. Hopkins and A. D. Hamilton, *J. Chem. Soc., Chem. Commun.*, 1995, 1251; (*d*) B. König, O. Möller and P. Bubenitschek, *J. Org.Chem.*, 1995, **60**, 4291; (*e*) H. Bock, T. T. H. Van, B. Solouki, G. Artus, E. Herdtweck and W. A. Herrmann, *Liebigs Ann. Chem.*, 1996, 403; (*f*) I. L. Karle, D. Ranganathan and V. Haridas, *J. Am. Chem. Soc.*, 1997, **119**, 2777; (*g*) C. Bielawski, Y.-S. Chen, P. Zhang, P.-J. Prest and J. S. Moore, *Chem. Commun.*, 1998, 1313; (*h*) M. Mazik, D. Bläser and R. Boese, *Tetrahedron*, 1999, **55**, 12771; (*i*) A. Zafar, S. J. Geib, Y. Hamuro, A. J. Carr and A. D. Hamilton, *Tetrahedron*, 2000, **56**, 8419; (*j*) N. Shan, A. D. Bond and W. Jones, *Tetrahedron Lett.*, 2002, **43**, 3101.

9 M. C. Etter and D. A. Adsmond, *J. Chem. Soc., Chem. Commun.*, 1990, 589.

10 I. L. Karle, D. Ranganathan and V. Haridas, *J. Am. Chem. Soc.*, 1996, **118**, 7128.

11 S. L. Johnson and K. A. Rumon, *J. Phys. Chem*, 1965, **69**, 74.

12 Z. Dega-Szafran, M. Gdaniec, M. Grunwald-Wyspiańska, Z. Kosturkiewicz, J. Koput, P. Krzyzanowski and M. Szafran, *J. Mol. Struct.*, 1992, **270**, 99.

13 A 1D network has one degree of translational symmetry and can be characterized by its rod group symmetry, whereas a 2D network with two degrees of translational symmetry can be characterized by its layer group symmetry; see : J. W. Lauher, Y.-L. Chang and F. W. Fowler, *Mol. Cryst. Liq. Cryst.*, 1992, **211**, 99.

14 A. Katrusiak, *J. Mol. Graphics Model.*, 2001, **19**, 363.

15 A. I. Kitaigorodskii, *Organic Chemical Crystallography*, Consultants Bureau, New York, 1961.

16 O. Kocian, N. Spencer, J. F. Stoddart, I. Cragg-Hine, M. Davidson, F. S. Mair, P. Raithby, R. Snaith, T. Kottke and E. Pohl, *Tetrahedron*, 1995, **51**, 579.

17 G. M. Sheldrick, *Acta Crystallogr., Sect. A*, 1990, **46**, 467.

18 G. M. Sheldrick, SHELXL-97. Program for the Refinement of Crystal Structures, University of Göttingen, Germany, 1997.